Imaging Science in Dentistry 2022; 52: 359-64
https://doi.org/10.5624/isd.20220077

Protrusion of the infraorbital canal into the maxillary sinus: A cross-sectional study in Cairo, Egypt

Salma Belal Eiid[1,2,*], Amani Ayman Mohamed[3]

[1]Department of Oral and Maxillofacial Radiology, Faculty of Dentistry, Cairo University, Cairo, Egypt
[2]Department of Oral and Maxillofacial Radiology, School of Dentistry, Newgiza University, Cairo, Egypt
[3]Department of Oral and Maxillofacial Radiology, Faculty of Dentistry, October 6 University, Giza, Egypt

ABSTRACT

Purpose: The aim of this study was to investigate the prevalence of infraorbital canal protrusion in an Egyptian subpopulation using cone-beam computed tomography and to describe its radiographic representation.

Materials and Methods: This retrospective cross-sectional study was conducted using the records of 77 patients and 123 maxillary sinuses. The full lengths of the sinuses were visible for the detection of infraorbital canal protrusion. The infraorbital canals were classified into 3 types based on their relation to the sinus. If the septum was present, its length and its distance from the sinus floor were measured. Qualitative and quantitative variables were described as percentages and means with standard deviations, respectively.

Results: The infraorbital canal most commonly presented as the normal confined type (detected in 78.1% of sinuses), whereas the suspended (or protruded) variant was found in 14.6% of the examined sinuses. The septal length ranged from 0.9 to 5.1 mm, with a mean of 2.8 ± 1.1 mm. The distance to the sinus floor ranged from 5.2 to 29.6 mm depending on the sinus shape and size.

Conclusion: The present study indicates that protrusion of the infraorbital canal is not rare, and surgeons that use the maxillary sinuses as corridors for their procedures must be more cautious, especially in the upper lateral confines of the sinus. ***(Imaging Sci Dent 2022; 52: 359-64)***

KEY WORDS: Cone-Beam Computed Tomography; Maxillary Sinus; Maxillary Nerve; Cranial Nerves

Introduction

Anomalous sinonasal cranial nerves can be encountered in the head and neck region, where they tend to deviate from the normal course by traversing adjacent air cavities, mimicking sinus septa. This phenomenon is usually associated with air cavity pneumatization or dehiscence of bony canal walls.[1]

Anomalous nervous anatomy has been reported in the sphenoid sinuses, with the optic, maxillary, or vidian nerves abnormally extending into the sphenoid sinus cavity.[2] Likewise, infraorbital nerve protrusion into the maxillary sinus has been documented.[1,3] The latter variant has recently become a topic of interest to ear, nose, and throat specialists and maxillofacial surgeons. This is due to the importance of a patent maxillary sinus in advanced sinonasal procedures such as Caldwell-Luc surgery, rhinoplasty, endoscopic sinus surgery, maxillary resection, and tumor removal from the maxilla and the maxillary sinus.[4]

The infraorbital nerve is the largest branch of the maxillary nerve, named based on its passage along the orbital floor.[5] The infraorbital anatomical complex originates from the inferior orbital fissure and terminates as the infraorbital foramen in the face. Its pathway includes the infraorbital groove and the infraorbital canal (IOC), which hold the infraorbital nerve and vessels.[5]

The infraorbital nerve is responsible for the sensory innervation of the zone extending from the lower eyelid to the upper lip. Normally, the nerve is covered with a thin layer of

Received April 25, 2022; Revised July 18, 2022; Accepted July 29, 2022
Published online September 7, 2022
*Correspondence to : Prof. Salma Belal Eiid
Department of Oral and Maxillofacial Radiology, Faculty of Dentistry, Cairo University, 11 El-Saraya St, Manial, Cairo, Egypt
Tel) 20-111-102-2226, E-mail) salma.eid@dentistry.cu.edu.eg

Imaging Science in Dentistry · pISSN 2233-7822 eISSN 2233-7830

bone, making it a fragile part of the orbital and maxillary sinus area. Damage to the infraorbital nerve is uncommon in normal circumstances. However, its aberrant suspension may predispose a person to iatrogenic complications due to nerve encroachment, such as hypoesthesia, paresthesia, and/or permanent soreness.[4,6,7] Therefore, a thorough radiological assessment of potential nerve protrusion is crucial before planning sinus surgery.[6,7] Computed tomography (CT) is widely utilized in sinonasal diagnostic procedures. Nevertheless, cone-beam computed tomography (CBCT) is often preferred by dentists and maxillofacial surgeons for maxillofacial imaging, due to its adequate spatial resolution and interactive display combined with sparing the patient the high radiation doses associated with CT scans.[7]

Previous studies of IOC anatomy were mainly conducted on skulls and cadavers using conventional imaging techniques.[8,9] Worldwide, few reports exist on the radiographic representation of the suspended IOC variant on cross-sectional imaging. A recently published systematic review clarified the different sinonasal variants, but lacked a comprehensive illustration of the variability of this infraorbital nerve variant.[3] Regarding geographical statistics, no published data were found on the Egyptian population. Therefore, the present study was designed to contribute further knowledge about this variant and to investigate the prevalence and radiological characteristics of infraorbital canal protrusion in a sample of Egyptians using CBCT.

Materials and Methods

Study design and population

In the reporting of this retrospective cross-sectional study, the RECORD statement - a checklist extended from the STROBE reporting guidelines for observational studies - was followed. Assuming an 8.8% prevalence of protruded IOCs (a figure based on the findings of Kalabalik et al.[7]), a total of 123 sinuses were needed for a margin of error of 5% and a 95% confidence interval. Sample size was calculated using Epi Info statistical software (version 7; Centers for Disease Control and Prevention, Atlanta, GA, USA).

The study was conducted at the Department of Oral and Maxillofacial Radiology of Cairo University using CBCT record scans from the radiology clinic's database, where newly registered patients are entered into the database by a maxillofacial radiologist with a minimum of 5 years of experience.

The CBCT records of patients who underwent CBCT imaging between 2019 and 2021 were collected. The CBCT scans were part of the patients' diagnostic and treatment plans. All scans were obtained using a Planmeca Promax Mid machine (Planmeca Oy, Helsinki, Finland) with a voxel size of 0.4 mm, current of 8/12.5 mA, and peak kilovoltage of 90 kVp. Romexis software (version 4.6.2.R, Planmeca Oy) was used for interpretation.

The patients ranged in age from 19 to 50 years. Images showing the full length of the maxillary sinus to the orbital rim were included. Images with hindering artifacts or visible maxillary abnormalities, pathologies, missing premolars or molars, or previous trauma were excluded. This computerized database search was thoroughly performed by a maxillofacial radiologist to select cases matching the preset criteria for age, field of view, and disease-free status.

Independent blinded reviewing of the IOCs was performed by 2 oral and maxillofacial radiologists with 5 and 10 years of experience to identify the presence or absence of the IOC variant. Equivocal cases were settled by consensus, and 1 of the radiologists was assigned to perform the linear measurements.

CBCT analysis and study variables

Case assessment was preceded by orientation of the cross lines, so that the hard palate was parallel to the axial plane and the nasal septum coincided with the sagittal plane. The primary outcome in this study was the prevalence of protruding IOCs in maxillary sinuses in Egyptians. The secondary outcomes focused on the length of the extended septum, its type, and the location of extension.

To detect IOC protrusion, the CBCT cuts were reviewed in the 3 orthogonal planes. The IOCs were categorized into 3 types based on the classification described by Ference et al.[4] in 2015. Type 1 indicates that the nerve canal is entirely contained within the sinus roof, type 2 that the nerve canal is below the roof but juxtaposes to it (Fig. 1), and type 3 that the nerve descends into the sinus and is suspended from the sinus roof with a septum (in other words, a protruding canal) (Fig. 2).

The IOC was considered to protrude into the maxillary sinus (type 3) if the entire wall of the IOC was not in contact with a maxillary sinus wall in any of the 3 planes. In contrast, if the entire circumference of the IOC was below the maxillary sinus wall but failed to exhibit compartmental separation of the sinus, this was categorized as type 2.

After the detection of IOC protrusion, the oblique cross-sections were adjusted to optimally measure the septal length. The septa were classified into 3 groups based on the system of Lantos et al.,[10] where class I, class II, or class III was assigned if the septal length was 1-3 mm, 3-7 mm, or ≥ 7 mm, respectively. As recommended by those authors,

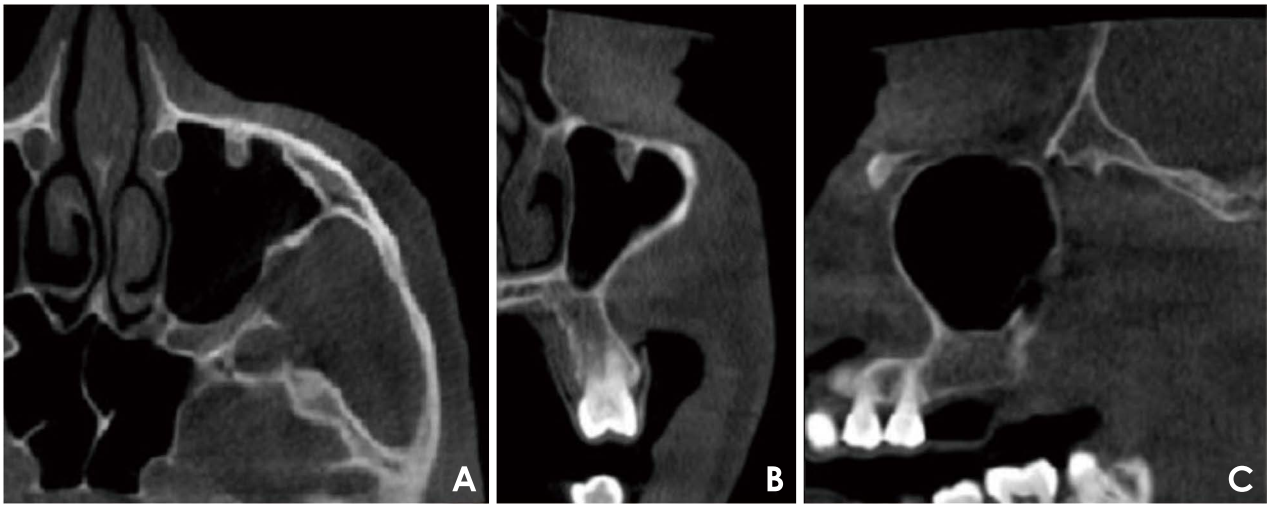

Fig. 1. Axial (A), coronal (B), and sagittal (C) cone-beam computed tomographic images show a type 2 infraorbital canal, where the canal extends beyond the confines of the sinus roof but with no obvious sinus compartmentalization in any plane.

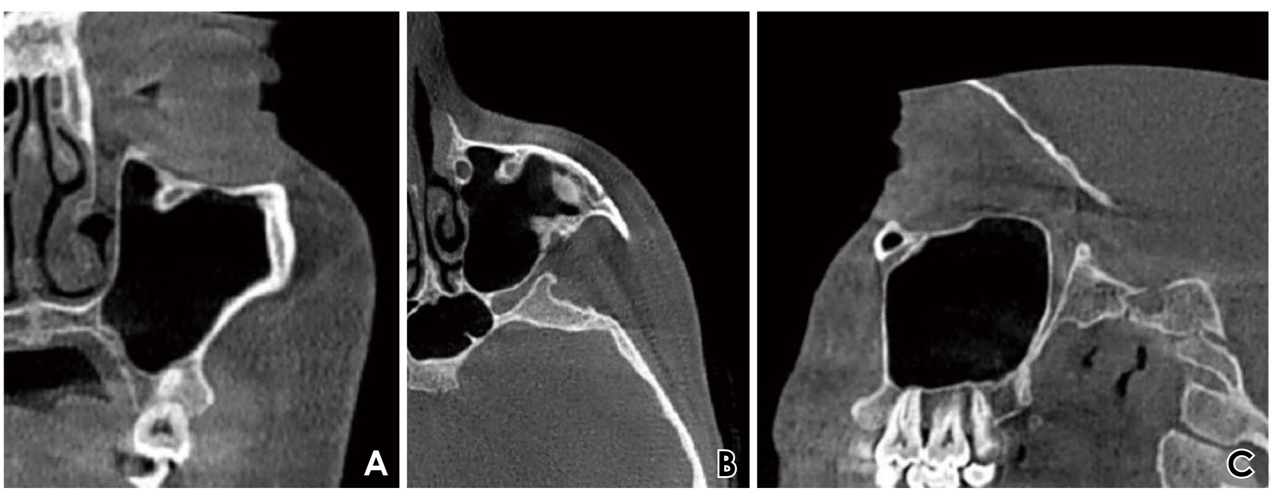

Fig. 2. Axial (A), coronal (B), and sagittal (C) cone-beam computed tomographic images reveal a type 3 infraorbital canal variant protruding into the sinus with a small compartment superior to the canal.

the length of the septum was measured on the axial plane from the maxillary sinus wall to the start of the suspended infraorbital foramen (Fig. 3).

On the coronal views for both type 2 and 3 variants, the distance from the end of the canal to the floor of the sinus was also measured. The coronal planes were chosen at the level of maximum protrusion of the IOC into the maxillary sinus (Fig. 4).

To spatially locate the protrusion within the sinus, the wall where the septum was hanging was registered as the anterior, lateral, medial, or posterior maxillary sinus wall. Then, the maxillary sinus was divided into thirds vertically and horizontally to pinpoint the location of the hanging septum.

Qualitative and quantitative variables were described as frequency (percentages) and means with standard deviations, respectively. Subgroup analyses for sex and side were not performed, since the sample size calculation was primarily based on the prevalence of the IOC variant and not on the sex and side representation patterns.

Results

The records of 81 patients were reviewed. Two contained motion artifacts, and 2 provided an incomplete view of the sinus roof. Therefore, a total of 77 patients (26 male, 51 female) and 123 sinuses were included. Table 1 depicts the

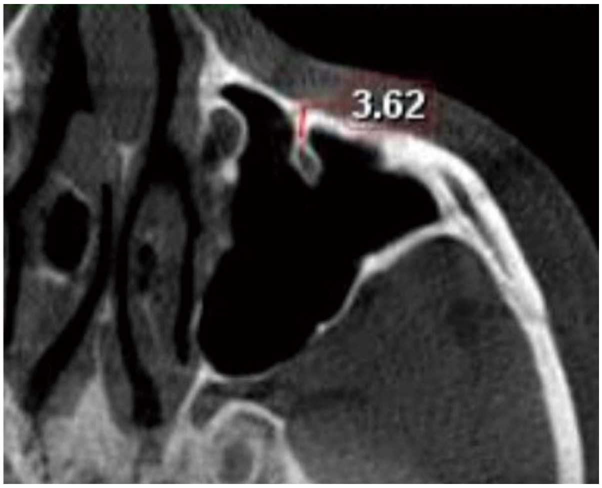

Fig. 3. Axial cone-beam computed tomographic image shows the horizontal suspension of the infraorbital canal with a displayed septal length of 3.6 mm, denoting a class II canal (septal length > 3 and ≤7 mm).

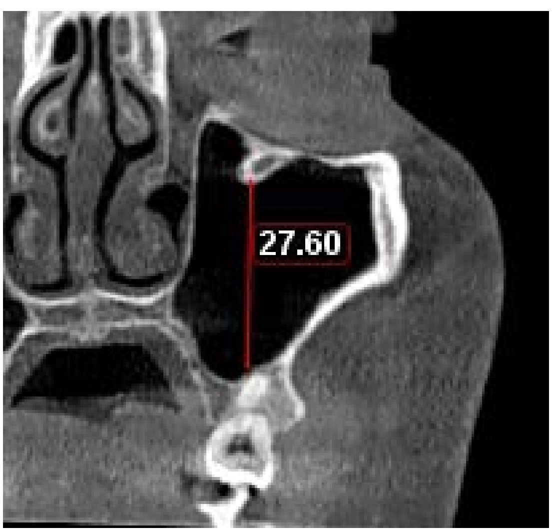

Fig. 4. Coronal cone-beam computed tomographic image reveals a hanging canal 27.6 mm from the sinus floor.

Table 1. Types and distributions of infraorbital canals

Classification	Type	Sinuses	
		Number	Percentage
Ference classification	Type 1	96	78.1%
	Type 2	9	7.3%
	Type 3	18	14.6%
	Total	123	100.0%
Lantos classification	Class I (≤3 mm)	10	56.0%
	Class II (>3 and ≤7 mm)	8	44.0%
	Class III (>7 mm)	0	0.0%
	Total	18	100.0%

different classifications of the IOC and their distributions within the sample. The most common type was the confined type 1, found in 78.1% (96 sinuses), followed by the protruded type 3 (14.6%, 18 sinuses); type 2 was the least common at 7.3% (9 sinuses).

The type 3 variants included 10 IOCs (56.0%) on the left side and 8 IOCs (44.0%) on the right side. Sex distribution analysis revealed only 2 men with type 3 variants; the rest were women (13 patients), 3 of whom had bilateral type 3 IOCs.

All protrusions originated from the anterior wall of the sinus. Over half (54.5%) of the protruded IOCs were found in the lateral third of the sinus, with fewer IOCs in the middle (36.4%) and medial (9.1%) areas.

The horizontal lengths of the protruded septa ranged from 0.9 to 5.1 mm, with a mean of 2.8 ± 1.1 mm. Per the classification system developed by Lantos et al.,[10] 10 cases (56.0%) were class I (1-3 mm), 8 cases (44.0%) were class II (>3 and ≤7 mm), and none were class III (>7 mm). All IOCs were found in the upper zone of the sinus, 5.2 to 29.6 mm from the maxillary sinus floor (mean distance, 15.8 ± 7 mm).

Discussion

In past years, research interest has focused on the superficial angles and landmarks of the IOC, which are required knowledge for proper local nerve blocks. More recently, the increase in access and navigation through the sinonasal area has required surgeons to better understand the internal anatomical variations that may be encountered.[4]

The presence of a cortical bony septum is known to be difficult for surgeons to bypass during sinus surgery; nerves and vessels enhance this difficulty. Therefore, explicit knowledge about such anatomic variations is crucial, and the discovery of a variant dictates a change in the treatment plan to avoid its violation.

The protruding IOC variant was reported by Mailleux et al.[11] in 2010 and by Elnil et al.[12] in 2014 as a very rare finding. Recent studies have revealed that this finding was not as rare as previously thought, with a prevalence in the literature ranging from 8.8% to 15.7%.[4-7,10,13]

The suspension of the IOC was classified by Ference et al.[4] into 3 main types according to the degree of protrusion. Later, Acar et al. proposed an amendment to this classification scheme[6] to add a fourth type, located at the outer limit of the zygomatic recess of the maxillary bone. Nevertheless, the former classification was chosen for the present study due to its straightforwardness.

In this study, the prevalence of the suspended IOC type 3 was 14.6%. This aligned with rates found in Iranian and Swiss subpopulations of 14.8%[14] and 15.7%[5], respectively. Two American and 1 Nepali subpopulation displayed lower rates of 10.8%,[4] 12.5%,[10] and 11.4%,[13] respectively. The lowest rates were cited by Turkish studies in 2020 and 2018 at 8.8%[7] and 9.5%,[6] respectively. This inconsistency in the prevalence of the IOC variant may be due to racial differences or sex- or age-based variability in sample selection between studies.

Interestingly, Stansfield et al.[15] in 2021 suggested a possible correlation between climate differences and the shape and size of the midface structures, including the sinuses. They revealed that groups in colder climates had larger sinuses than those in warm climates. Based on this theory, the variability in the literature regarding rates of the protruding IOC may be attributable to climate differences. However, further investigations are required to clarify the relationships of climate and ethnicity with its occurrence.

In the present study, the length of the IOC septum was measured to showcase the clinical impact of the horizontal suspension of this nerve in the maxillary sinus, where the further the canal into the sinus, the greater the risk.

With this in mind, over half of the study participants had septa of less than 3 mm, and none exceeded 7 mm (mean length, 2.8 ± 1.1 mm). In previous studies, the mean septal lengths were reported to be longer, at 4.9 mm (ranging from 0.9 to 8.9 mm with 3 cases exceeding 7 mm),[13] 4 mm (ranging from 1 to 11 mm with 10 cases exceeding 7 mm),[10] and 3.8 mm (ranging from 1.3 to 10.1 mm).[7] The shorter septa in the present study may be due to the high proportion of women, who have smaller sinuses with shorter septal suspension, in the sample. Discrepancies in measurement methodologies among previous studies hindered further comparisons.[4,14]

To the knowledge of these authors, only 1 study, conducted by Kalabalik et al.,[7] has assessed the position of the IOC variant relative to the sinus floor; the results revealed long distances (mean, 25.4 mm; range, 14.2 mm to 36.4 mm). An assessment of this relationship in the present study showed that the descending aberrant canal in the sinus carries little risk in simple dental procedures such as extractions and implant placements, where the nearest canal was 5.2 mm from the floor. However, in more extensive surgery, surgeons must be more cautious during sinus navigation, especially in small maxillary sinuses.

The wide range of distances to the sinus floor in this study was due to the size and shape variations of the maxillary sinuses and the irregular festooning of the sinus borders. Most protrusions were largely located in the upper lateral third, with fewer found in the medial and middle portions of the sinus. Laterally oriented septa were nearer to the floor, conforming with the triangular sinus shape. Therefore, surgeons should understand that accessing the sinus through the upper lateral confines may be a high-risk procedure.

Based on the study results, IOC protrusion is not a rare finding, and radiologists should be more knowledgeable about this manifestation. A routine preoperative checkup for this area should be provided when surgery is under consideration. Future large-scale studies are needed for subgroup analyses of age-, sex-, and side-based variability. Furthermore, a detailed systematic review assessing the relationships of climate, race, and ethnicity with this challenging variant will be valuable.

Conflicts of Interest: None

References

1. Farina D, Lombardi D, Bertuletti M, Palumbo G, Zorza I, Ravanelli M. An additional challenge for head and neck radiologists: anatomic variants posing a surgical risk - a pictorial review. Insights Imaging 2019; 10: 112.
2. Singh A, Manjunath K, Singh H. Relationship of sphenoid sinus to adjacent structures in South India: a retrospective cross sectional study. Egypt J Otolaryngol 2022; 38: 8.
3. Papadopoulou AM, Chrysikos D, Samolis A, Tsakotos G, Troupis T. Anatomical variations of the nasal cavities and paranasal sinuses: a systematic review. Cureus 2021; 13: e12727.
4. Ference EH, Smith SS, Conley D, Chandra RK. Surgical anatomy and variations of the infraorbital nerve. Laryngoscope 2015; 125: 1296-300.
5. Fontolliet M, Bornstein MM, von Arx T. Characteristics and dimensions of the infraorbital canal: a radiographic analysis using cone beam computed tomography (CBCT). Surg Radiol Anat 2019; 41: 169-79.
6. Açar G, Özen KE, Güler İ, Büyükmumcu M. Computed tomography evaluation of the morphometry and variations of the infraorbital canal relating to endoscopic surgery. Braz J Otorhinolaryngol 2018; 84: 713-21.
7. Kalabalık F, Aktaş T, Akan E, Aytuğar E. Radiographic evaluation of infraorbital canal protrusion into maxillary sinus using cone-beam computed tomography. J Oral Maxillofac Res 2020; 11: e5.
8. Yesilova E, Bayrakdar IS. The appearance of the infraorbital canal and infraorbital ethmoid (haller's) cells on panoramic radiography of edentulous patients. Biomed Res Int 2018;

2018: 1293124.
9. Shin KJ, Lee SH, Park MG, Shin HJ, Lee AG. Location of the accessory infraorbital foramen with reference to external landmarks and its clinical implications. Sci Rep 2020; 10: 8566.
10. Lantos JE, Pearlman AN, Gupta A, Chazen JL, Zimmerman RD, Shatzkes DR, et al. Protrusion of the infraorbital nerve into the maxillary sinus on CT: prevalence, proposed grading method, and suggested clinical implications. AJNR Am J Neuroradiol 2016; 37: 349-53.
11. Mailleux P, Desgain O, Ingabire MI. Ectopic infraorbital nerve in a maxillary sinus septum: another potentially dangerous variant for sinus surgery. JBR-BTR 2010; 93: 308-9.
12. Elnil H, Al-Tubaikh JA, El Beltagi AH. Into the septum I go, a case of bilateral ectopic infraorbital nerves: a not-to-miss preoperative sinonasal CT variant. Neuroradiol J 2014; 27: 146-9.
13. Gautam R, Adhikari D, Dhital M, Thakur S, Adhikari B. The prevalence of protrusion of infraorbital nerve into maxillary sinus identified on CT scan of the paranasal sinuses at a tertiary hospital in Nepal. Nepal J Radiol 2018; 8: 7-12.
14. Haghnegahdar A, Khojastepour L, Naderi A. Evaluation of infraorbital canal in cone beam computed tomography of maxillary sinus. J Dent (Shiraz) 2018; 19: 41-7.
15. Stansfield E, Mitteroecker P, Vasilyev SY, Vasilyev S, Butaric LN. Respiratory adaptation to climate in modern humans and Upper Palaeolithic individuals from Sungir and Mladeč. Sci Rep 2021; 11: 7997.